
POTENTIODYNAMIC BEHAVIOUR OF TIN ELECTRODE IN SOME CARBOXYLIC ACIDS SOLUTIONS

R. M. ABOU SHAHBA, A. S. I. AHMED, E. M. ATTIA AND A. E. EL-SHENNAWY

Chemistry Department, Faculty of Science (for Girls), AL- Azhar University, Nasr City, Cairo, Egypt

Abstract

Potentiodynamic behaviour of tin electrode in citric, oxalic, maleic and malic acids was studied at room temperature. The various electrochemical parameters were calculated. In addition, the metallographic structure of tin surface electrode was examined for some solutions using scanning electron microscope (SEM). The anodic E/I curves were characterized by active - passive transition state. The anodic active region was due to the formation of soluble Sn(II) species. The passivity of tin anode was related to the hydrolysis of Sn(IV) and precipitation of Sn(OH)₄ film on the anode surface. The addition of different percentages of sucrose to (1 M) of all organic acids used inhibited the anodic dissolution of tin electrode and enhanced the attainment of passivity. While the addition of sodium chloride accelerated the corrosion of tin and delayed the establishment of passivation. In citric, maleic and malic acids, inhibition was of mixed type and occurred by adsorption of SnL complex molecules following the Temkin isotherm. In case of oxalic acid the inhibition was found to be predominantly anodic occurring by adsorption of SnL₂ complex and following the Langmuir isotherm.

Introduction

The electrochemical behaviour of tin is of interest due to its widespread technology applications. A relatively large amount of work has focused on the electrochemical behaviour of the metal in the presence of organic acids. These acids are naturally present in canned food and therefore they participate directly in the electrochemical corrosion and/or passivation of the metal⁽¹⁾. The resistance of tinned plate towards corrosion is related to the interrelationship of the characteristics of can and the product packed therein⁽²⁾. Therefore, the corrosion behaviour of tin in the presence of fruit acids had attracted much attention^(3,4).

Corrosion behaviour of organic acid solutions is studied in oxalic, citric and tartaric acids in the pH range 2- 6 and illustrated that, increasing the concentration caused increasing the rate of corrosion⁽⁵⁾. The polarization curves exhibited two anodic peaks. The height of peak increased with increasing solution pH and temperature⁽⁶⁾.

Using electron microscope technique in addition to the potentiodynamic method, the film growing process in 0.5 M citric acid solution followed a dissolution precipitation mechanism⁽⁷⁾. The E/I curves of citric and maleic acids exhibited an active/passive transition^(8,9). In citrate buffer solutions, primary passivation is due to the formation of Sn(II)-containing surface film. During secondary passivation direct oxidation of Sn to Sn(IV) takes place, either as soluble ions or as a hydroxide layer⁽¹⁰⁾. In maleic acid solutions, the dissolution process is controlled partly by diffusion of the solution species. The passivity is due to the presence of thin film of SnO₂ on the anode surface formed by dehydration of precipitated Sn(OH)₄⁽⁹⁾. In tartaric acid solutions, passivation is due to formation of Sn(OH)₄ and/or SnO₂ film on the anode surface⁽¹¹⁾.

In a synthetic medium similar to industrial water, the increasing of temperature in the range of 20- 70°C accelerates the corrosion process⁽¹²⁾. While addition of oxo-anions leads to retard a breakdown of passivation and the inhibition of pitting process of tin⁽¹³⁾. The growth of an inert phase at the interface, the deposition of a surface organic layer or the eventual modification of the surface electronic properties may give rise to surface passivation⁽¹⁴⁾.

The object of the present work is the study of the anodic behaviour of tin electrode in carboxylic acids such as: oxalic, citric, maleic and malic acids solutions by potentiodynamic method. Moreover, investigating the effect of presence of some selected compounds as inhibitors.

Experiment

The material used in the present study was spectroscopically pure tin rod electrode (99.999 % pure) with a surface area of 2 cm². Prior to each experiment, the surface was prepared by polishing with different grades emery papers, then diamond paste (1µm), washing by distilled water, drying and quickly inserting in the electrochemical cell. The counter electrode was a platinum sheet, and the reference electrode was a compact saturated calomel electrode.

Anodic and cathodic potentiodynamic polarization scans were performed with electronic potentiostat (Volt Lab PGZ 301 Dynamic EIS Voltammetry). All measurements were performed in freshly prepared solutions at room temperature. The anodic E/I curves for all solutions were swept from -1.5 to +1.5 V at scan rate of 20 mV/s.

Morphology of tin electrode surface is studied using scanning electron microscope (SEM), JOEL, JSM- T 20, Japan.

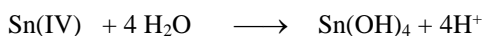
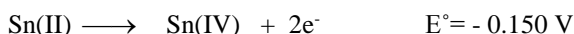
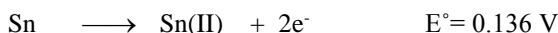
Results And Discussion

Behaviour of tin electrode in different concentrations of organic acids solutions

The E/I profile of citric acid exhibits an active- passive behaviour for all concentrations. The active dissolution region involves anodic peak (except at 2M) followed by passive region which extends up to 1.5 V with no sign for oxygen evolution (Figure 1).

It is observed from the curves that an increase in acid concentration increases i_{corr} of the anodic peak, indicating that the citrate ions accelerated the dissolution of tin. This effect can be due to the adsorption of citrate ions (L^{2-}) on the electrode surface and to the formation of soluble complex species (SnL)^(3, 15, 16). Also an increase of the citric acid concentration shifts its peak potential ($E_{corr.}$) to more positive values. Maleic acid behaves similarly but the passive region is extended up to 1.5 V with almost constant current density.

The anodic active dissolution in maleic acid is due to formation of soluble Sn^{2+} species, which is subsequently oxidized to Sn^{4+} . The passivity of tin electrode is due to the hydrolysis of Sn^{4+} and precipitation of $Sn(OH)_4$ on the electrode surface. The dissolution process could be represented by the following equations⁽¹⁷⁾:



$Sn(OH)_4$ is highly insoluble as its solubility product is 1×10^{-95} which precipitates giving rise to a passivation film.

Dehydration of $Sn(OH)_4$ layer resulted in the formation of more stable SnO_2 film.



For this dehydration reaction ΔG is -42 KJ mol^{-1} ⁽¹⁸⁾. Therefore, the formation of SnO_2 species is thermodynamically favoured. When the surface is covered with SnO_2 film, the current density falls to i_{pass} value. Therefore, one can conclude that passivity is due to the formation of SnO_2 film on tin electrode surface. In a solution containing a dibasic acid as maleic acid which represented by H_2L , there are three possible ligands: H_2L , HL^- and L^{2-} , and the complex could contain many contributions of these ligands⁽¹⁸⁾.

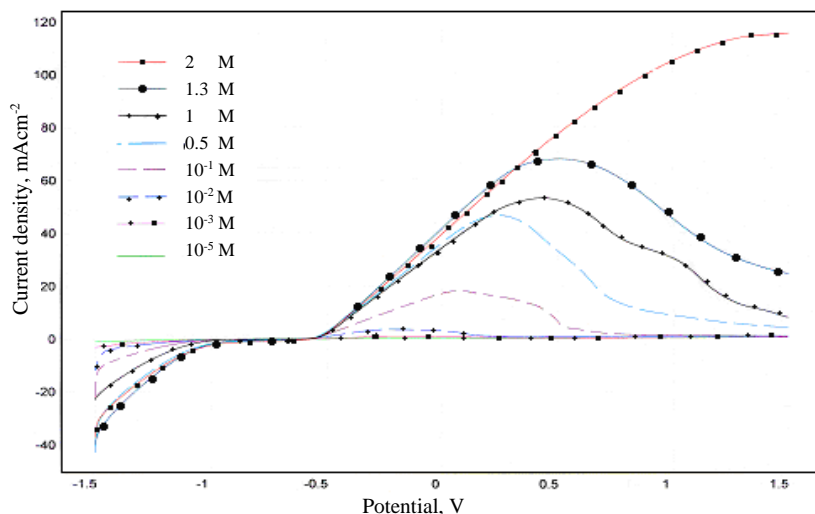


Figure (1): Potentiodynamic polarization curves of tin electrode in different concentrations of citric acid solutions

Oxalic acid behaves similarly but with a sharp peak which at low concentrations disappeared (Figure 2). The passivation in oxalic acid is found to occur via monolayer chemisorptions of the $\text{SnL}_2^{(15)}$ complex anions at anodic sites, conforming approximately to the Langmuir isotherm⁽¹⁹⁾.

In malic acid, there is one anodic peak at 0.5 M while in other concentrations the peak completely disappeared and no passivation of tin electrode is observed.

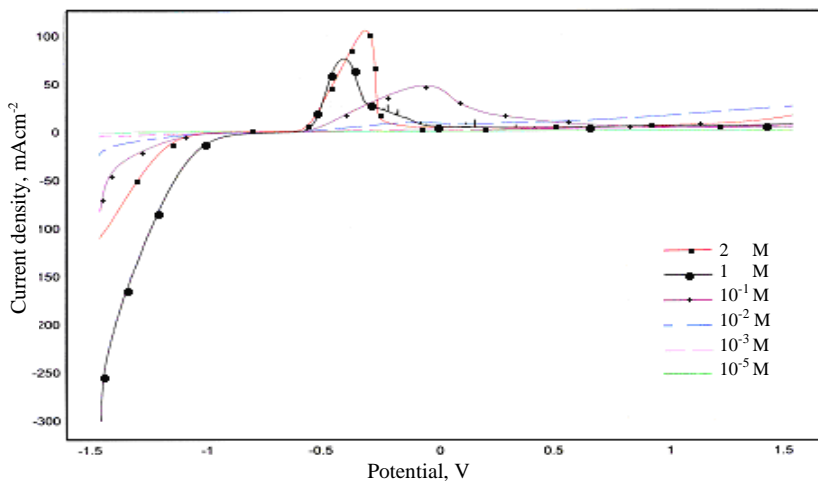


Figure (2): Potentiodynamic polarization curves of tin electrode in different concentrations of oxalic acid solutions

Adsorption isotherms for the SnL complexes in tartaric, malic and citric acids follow that of Temkin, which characterizes the chemisorption of uncharged substances on heterogeneous surfaces ⁽¹⁹⁾.

Values of corrosion rate in millimeter per year (mm/y) are calculated from i_{corr} values as shown below ⁽²⁰⁾.

$$\text{Corrosion rate} = \Delta E / \Delta i \approx R_p = B_a \cdot B_c / 2.3 i_{\text{corr}} (B_a + B_c)$$

Where:

$\Delta E / \Delta i$ = the slope of the linear region, equal the polarization resistance R_p .

ΔE and Δi are expressed in (V) and (mA / cm²) respectively.

i_{corr} = Corrosion current (mA / cm²). B_a and B_c = anodic and cathodic Tafel constants, respectively (in mV/decade).

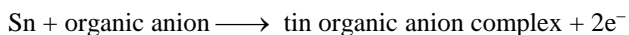
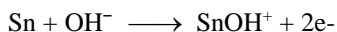
The electrochemical parameters are tabulated in Table (1). The results revealed that, the corrosion current i_{corr} and corrosion rate increased as the concentration increased for all acids studied. Corrosion potential became more positive by increasing the acid concentration except for oxalic acid. This behaviour may be attributed to the formation of tin complexes with the organic acid anions acting as ligands, which in turn reduces the tin activity in solution and results in a change in the corrosion potential in the active direction followed by an increase in the corrosion rate ⁽⁵⁾.

Morphology of tin electrode surface in 1 M citric and oxalic acids solutions is studied using scanning electron microscope. The specimen revealed a highly etched surface with some scattered pits. In oxalic acid, the formed passive layer is adherent, while in citric acid the passive layer is spongy (Figures 3, 4).

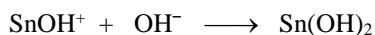
Effect of inorganic additive, NaCl

Addition of Cl⁻ ions to citric acid made the curves clearly different where there are no anodic peak occurred (Figure 5). Maleic and malic acids behaved similarly as citric acid.

In oxalic acid there are two anodic peaks in presence of Cl⁻ ions. The charge transfer reaction occurs in the first active dissolution peak resulting in the formation of tin ions. The charge is used to produce the following soluble species:



However, when the concentration of the complex SnOH⁺ exceeds the solubility product of Sn(OH)₂, the latter precipitates on the electrode surface:



Thus i_{corr} drops suggesting the onset of primary passivation at potential comparable with the equilibrium potential of the system Sn/Sn(OH)₂. During the potential sweep to positive direction and in the presence of Cl⁻ ions, Sn(OH)₂ starts to dissolve. Subsequently, current density increases again up to the second peak.

Table (1): The electrochemical parameters of tin electrode in different concentrations of organic acids

Acid Solution	Conc. M	E _{corr.} mV	i _{corr.} mA/cm ²	Tafel Slopes (mV/decade)		Corrosion rate mm/y
				B _a	B _c	
Citric	2.0	-568.1	0.315	116.1	-464.0	3.740
	1.3	-576.1	0.348	123.8	-821.0	4.130
	1.0	-880.4	0.313	116.0	-464.8	3.700
	5x10 ⁻¹	-579.4	0.240	122.9	-505.9	2.870
	1x10 ⁻¹	-586.0	0.244	161.4	-153.3	2.890
	1x10 ⁻²	-608.5	0.100	139.1	-478.7	1.180
	1x10 ⁻³	-618.8	0.102	287.5	-620.7	1.210
Oxalic	1x10 ⁻⁵	-637.5	0.005	287.5	-620.7	0.330
	2.0	-692.6	0.380	44.5	-274.0	4.560
	1.0	-655.8	0.232	85.9	-414.0	2.754
	1x10 ⁻¹	-640.7	0.208	92.8	-490.0	2.470
	1x10 ⁻²	-638.0	0.239	150.0	-470.0	2.843
	1x10 ⁻³	-634.0	0.204	302.0	-350.0	2.428
Maleic	1x10 ⁻⁵	-611.1	0.100	352.0	-324.0	0.125
	2.0	-501.0	3.780	135.9	-220.0	44.850
	1.5	-504.0	3.605	137.8	-186.0	42.780
	1.0	-516.7	3.130	118.9	-158.9	37.180
	5x10 ⁻¹	-519.1	2.100	150.5	-212.6	25.590
	1x10 ⁻¹	-510.4	0.480	125.0	-216.9	5.804
	1x10 ⁻²	-568.9	0.140	137.1	-304.2	1.673
	1x10 ⁻³	-552.5	0.086	344.8	-413.6	1.028
Malic	1x10 ⁻⁵	-618.6	0.005	318.7	-347.0	0.070
	2.0	564.7	0.691	156.7	-344.6	8.200
	1.5	-574.4	0.447	149.7	-350.0	5.300
	1.0	-576.8	0.203	110.4	-229.5	2.400
	5x10 ⁻¹	-583.9	0.216	169.7	-393.8	2.560
	1x10 ⁻¹	-584.8	0.103	94.5	-295.0	1.220
	1x10 ⁻²	-571.7	0.097	212.3	-520.0	1.160
	1x10 ⁻³	-573.8	0.096	317.3	-391.9	1.150
1x10 ⁻⁵	-564.0	0.006	336.4	-355.0	1.120	

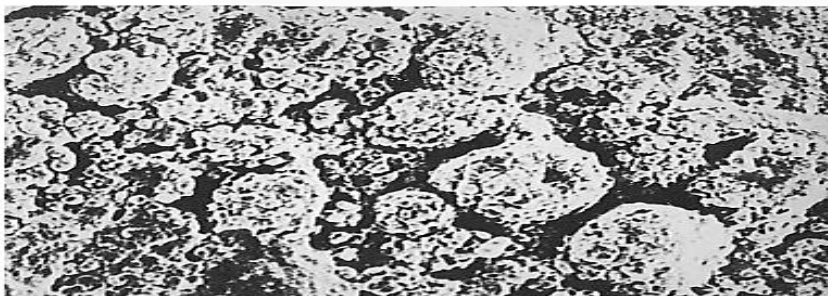


Figure (3): SEM micrograph for tin electrode in (1 M) citric acid (X 1000)

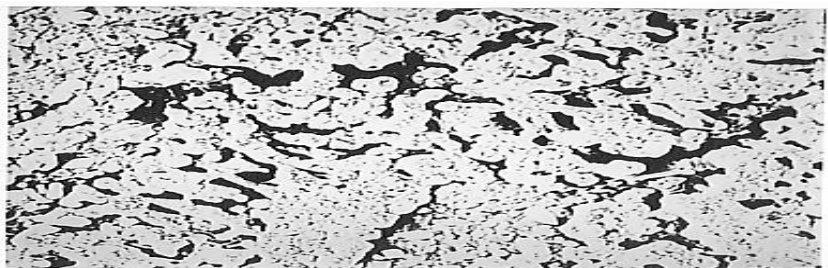


Figure (4): SEM micrograph for tin electrode in (1 M) oxalic acid (X 1000)

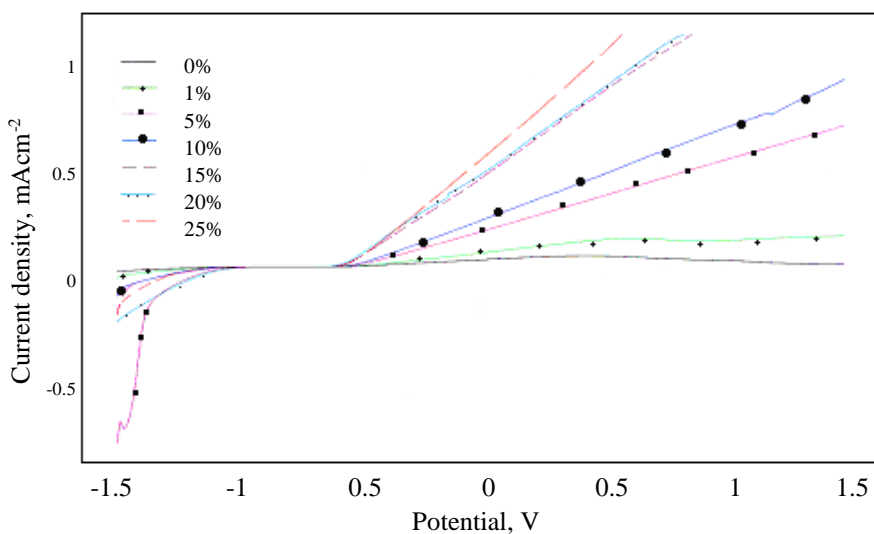


Figure (5): Potentiodynamic polarization curves of tin electrode in 1 M citric acid containing various % of Cl⁻ ions.

The recorded results of the electrochemical parameters show that, the corrosion of tin electrode in 1 M test solutions increased with increasing concentration of NaCl. This indicated that Cl^- ions accelerate the active dissolution of tin electrode and tend to breakdown the passive layer. The oscillations observed in Figure (6) can be attributed to the competition between the anodic formation and chemical dissolution of the oxide film on the electrode surface.

The highest values of corrosion rate are observed for maleic acid while the lowest ones are recorded for malic acid (Table 2).

Effect of organic additive, sucrose

The inhibitor efficiency (I.E.) is calculated from the polarization method using the following equation ⁽²¹⁾:

$$\text{I.E. \%} = (\text{C.R.})_{\text{uninh.}} - (\text{C.R.})_{\text{inh}} / (\text{C.R.})_{\text{uninh.}} \times 100$$

Where: $(\text{C.R.})_{\text{inh}}$ and $(\text{C.R.})_{\text{uninh}}$ are the corrosion rate with and without inhibitor, respectively. Addition of sucrose strongly inhibits the active dissolution of tin electrode in malic acid since it had the highest inhibition efficiency value (I.E. = 99.2 % at 25 % sucrose in 1 M malic acid). The lowest values are observed for maleic acid (Table 3).

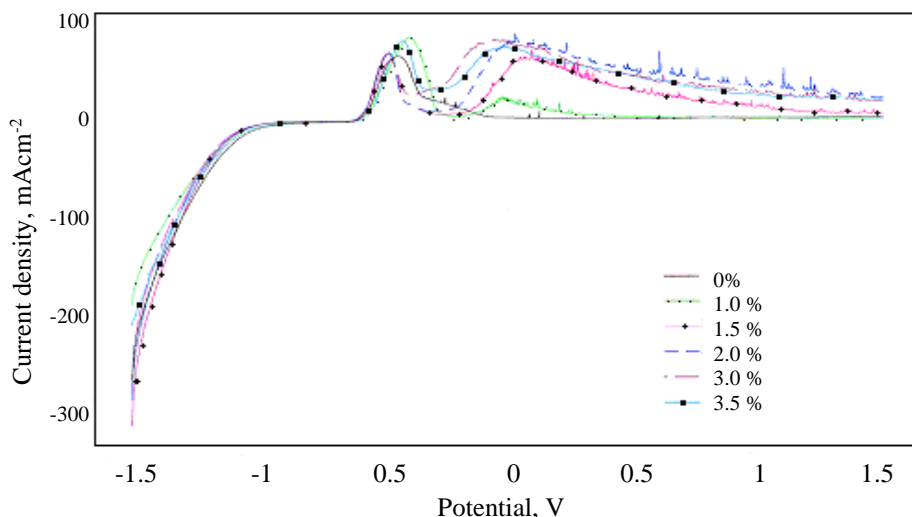


Figure (6): Potentiodynamic polarization curves of tin electrode in 1 M oxalic acid containing various % of Cl^- ions.

Table (2): The electrochemical parameters of tin electrode in 1 M acids solutions containing various % of Cl⁻ ions

Acid Solution	% NaCl	E _{corr.} mV	i _{corr.} mA/cm ²	Tafel Slopes (mV/decade)		Corrosion rate mm/y
				B _a	B _c	
Citric	0 %	-580.4	0.310	116.1	-464.8	3.7
	1%	-915.0	0.500	84.4	-544.9	6.9
	5 %	-942.8	0.698	181.5	-154.1	8.3
	10%	-994.0	0.700	284.6	-164.6	9.0
	15%	-999.0	0.817	217.9	-124.3	9.7
	20 %	-1009.0	0.924	228.2	-152.1	10.9
	25%	-1013.0	1.018	284.3	-164.3	12.1
Oxalic	0 %	-655.8	0.232	85.9	-414.5	2.8
	1%	-662.0	0.600	142.6	-143.6	8.0
	1.5 %	-679.0	0.650	213.4	-146.0	8.4
	2 %	-688.0	0.690	47.8	-155.0	9.0
	3 %	-700.7	0.730	44.5	-119.3	9.7
	3.5 %	-710.0	0.800	70.7	-295.5	10.3
Maleic	0 %	-516.1	3.130	118.9	-158.9	37.2
	1%	-534.0	9.180	204.7	-313.9	108.9
	5 %	-538.0	15.240	132.2	-216.4	162.2
	10%	-542.0	24.830	121.1	-226.5	257.3
	15%	-546.0	36.690	258.8	-193.4	435.3
	20 %	-590.0	36.800	252.4	-167.1	436.6
	25%	-590.0	38.900	274.4	-209.2	462.0
Malic	0 %	-576.8	0.203	110.4	-229.5	2.4
	1%	-607.0	0.260	62.5	-122.4	3.1
	5 %	-671.1	0.280	164.8	-174.3	3.3
	10%	-687.0	0.290	227.9	-224.0	3.5
	15%	-741.0	0.300	57.1	-367.5	3.8
	20 %	-995.5	0.300	393.1	-154.7	3.7
	25%	-991.0	0.400	308.2	-157.1	5.6

The inhibition efficiency increased by increasing the sucrose percentage, while the corrosion rate decreased for all organic acids solutions. This indicated that the presence of sucrose inhibits the anodic dissolution of tin electrode. The inhibitive effect might be due to the adsorption of ions on the metal surface.

The effect of 25 % of sucrose on the morphology of tin electrode surface in (1M) citric and oxalic acids is studied by SEM. It is clear from Figures (7 and 8) that sucrose is adsorbed on the surface of tin electrode forming a good protective film present on the tin surface. This confirms the highest inhibition efficiency of sucrose. As a result, sucrose can be used as inhibitor for organic acids to reduce the aggressiveness of these acids and also as additive to improve the surface conditions of the tin electrode.

Table (3): The electrochemical parameter of tin electrode in 1M acids solutions containing various % of sucrose

Acid Solution	% Sucrose	$E_{corr.}$ mV	$i_{corr.}$ mA/cm ²	Tafel Slopes, (mV/decade)		Corrosion rate mm/y	I.E. %
				B _a	B _c		
Citric	0 %	-580.4	0.310	116.1	-464.8	3.700	—
	1%	-578.0	0.271	132.5	-646.8	3.221	12.50
	10 %	-577.7	0.256	131.5	-551.9	3.036	17.40
	15 %	-579.0	0.214	133.2	-606.0	2.540	30.96
	20%	-576.0	0.210	92.2	-528.3	2.520	32.25
	25 %	-569.4	0.183	145.5	-515.5	2.170	40.96
Oxalic	0 %	-655.0	0.232	85.9	-414.5	2.754	—
	1%	-648.1	0.200	175.0	-191.6	2.463	13.70
	10 %	-681.0	0.110	61.0	-239.7	1.305	52.50
	15 %	-713.0	0.029	60.4	-130.2	0.345	87.50
	20%	-731.9	0.021	68.3	-155.0	0.258	90.90
	25 %	-762.7	0.020	82.9	-150.0	0.240	91.30
Maleic	0 %	-516.1	3.130	118.9	-158.9	37.180	—
	1%	-515.9	3.020	226.5	-286.1	36.500	3.50
	5 %	-515.8	2.930	184.1	-254.3	35.800	6.30
	10 %	-515.7	2.850	181.8	-250.6	35.200	8.90
	15 %	-515.7	2.800	166.1	-233.8	34.700	10.50
	20%	-513.1	2.760	176.6	-245.2	34.200	11.80
	25 %	-513.0	2.730	200.9	-271.6	34.000	12.70
Malic	0 %	-576.8	2.030	110.4	-229.5	2.408	—
	1 %	-570.9	0.100	112.3	-260.8	1.230	50.73
	5 %	-556.5	0.008	51.6	-94.6	0.095	96.05
	10 %	-542.7	0.006	61.8	-89.0	0.072	96.99
	15 %	-540.5	0.005	63.9	-96.9	0.057	97.50
	20%	-535.1	0.002	49.0	-127.8	0.027	98.80
	25 %	-530.2	0.002	54.9	-163.7	0.014	99.20

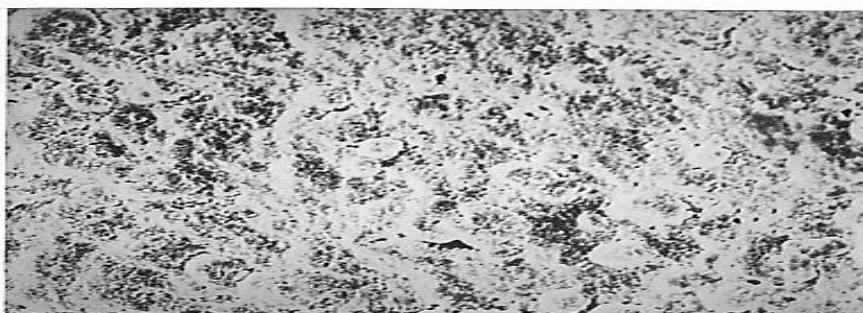


Figure (7): SEM micrograph for tin electrode in (1 M) citric acid inhibited with 25 % sucrose (X 1000)

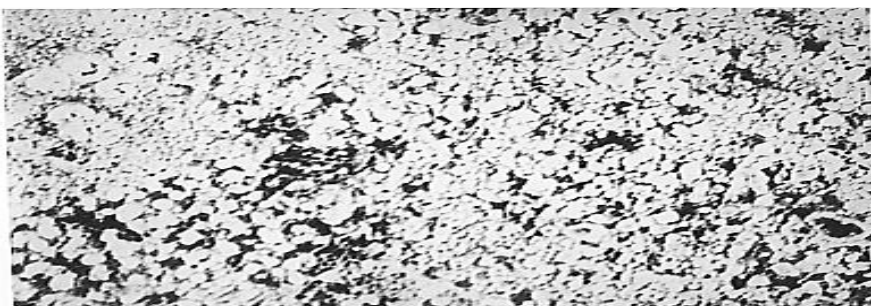


Figure (8): SEM micrograph for tin electrode in (1 M) oxalic acid inhibited with 25 % sucrose (X 1000)

Effect of some salts of acids on the behaviour of tin electrode

Figure (9) shows that, the addition of low concentrations of trisodium citrate anions to 1 M citric acid strongly inhibits the active dissolution of tin electrode since the peak current - density decreases and its corresponding peak potential shifts to more negative direction with adding further amounts of citrate.

On the other hand, by the addition of higher concentrations of citrate anions (1- 2 M), two anodic peaks are established. Thus citrate can cause partial dissolution of the oxide film that formed when tin surface is exposed to air ^(4, 22).

In oxalic acid, the decrease in corrosion rate as well as i_{corr} by increasing the amount of potassium oxalate was associated with an increase in the positive shift of corrosion potential (Figure 10). This behaviour denotes inhibition of the mixed type and suggests a predominant anodic effect.

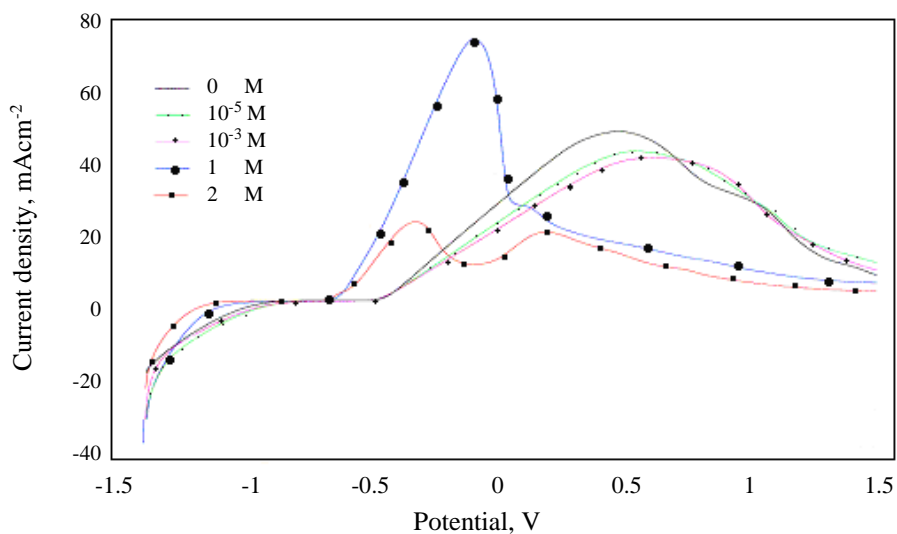


Figure (9): Potentiodynamic anodic and cathodic polarization curves of tin electrode in 1M citric acid with different concentrations of citrate ions.

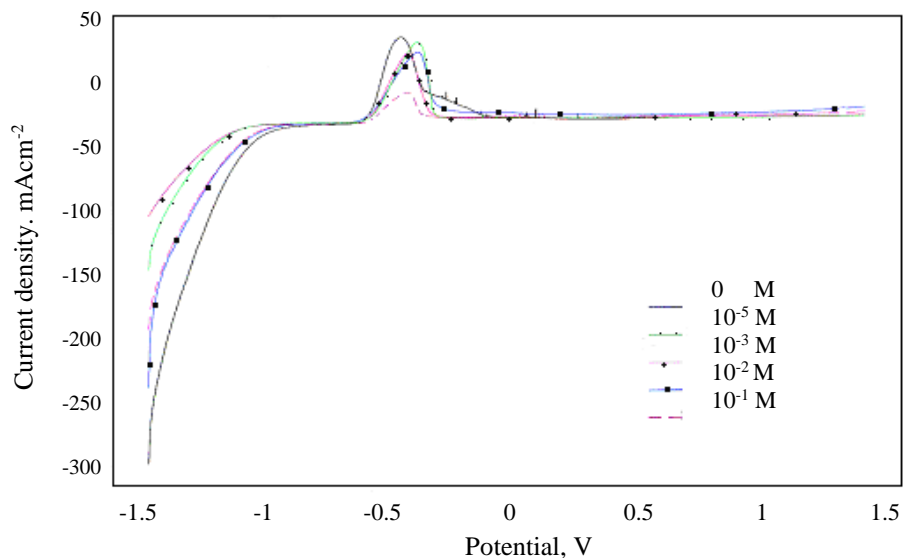


Figure (10): Potentiodynamic anodic and cathodic polarization curves of tin electrode in 1M oxalic acid with different concentrations of oxalate ions.

Table (4): The electrochemical parameters of tin electrode in 1M of citric and oxalic acids with different concentrations of their salt solutions

Test solution	Additive M	$E_{\text{corr.}}$ mV	$i_{\text{corr.}}$ mA/cm ²	Tafel Slopes (mV/decade)		Corrosion rate mm/y	I.E %
				B_a	B_c		
Citric + citrate	—	-580.4	0.310	116.1	-464.8	3.700	—
	10 ⁻⁵	-596.6	0.250	113.1	-347.9	3.018	19.3
	10 ⁻³	-596.9	0.240	93.9	-461.0	3.000	22.5
	1	-785.0	0.060	50.6	-319.4	1.800	80.6
	2	-997.0	0.016	239.7	-137.8	1.026	94.8
Oxalic + oxalate	—	-655.8	0.232	85.9	-414.5	2.754	—
	10 ⁻⁵	-649.0	0.243	386.3	-141.6	2.891	4.7
	10 ⁻³	-630.0	0.173	207.7	-142.6	2.057	25.0
	10 ⁻²	-611.6	0.174	310.9	-148.0	2.071	25.0
	10 ⁻¹	-604.0	0.117	53.2	-379.9	1.394	49.0

As clear from Table (4), inhibition efficiency (I.E.%) increased with the increasing of additive salt concentration studied.

Conclusion

The anodic behavior of tin in some carboxylic acid solutions (citric, oxalic, maleic and malic) were examined by potentiodynamic polarization technique. The inhibition of tin in oxalic acid was found to be predominantly anodic and occurred via monolayer chemisorption of the SnL₂ complex anion at anodic sites, confirming approximately with the Langmuir isotherm. While the inhibition in other three acids was found to be of the mixed type and occur via chemisorption of the SnL complex at both anodic and cathodic sites following the Temkin isotherm. The corrosion rate of tin electrode increased as the concentration of all organic acids studied increased.

Cl⁻ ions accelerate the active dissolution and tend to break down the passive layer. While sucrose can be used as inhibitor for organic acids studied and also as additive to improve the surface conditions of the tin electrode.

Inhibition efficiency of citric and oxalic acids increased with increasing of citrate and oxalate concentrations studied.

References

1. C. M. V. B. ALMEIDA, T. RABOCZKAY AND B. F. GIANNETTI; Journal of Applied Electrochemistry, 29(1) pp. 123 (1999).
2. A. R. WILLEY; Br. Corrosion J., 7 pp. 29 (1972).

3. B. F. GIANNETTI, P. T. SUMODJO, AND T. RABOCKAI; *Journal of Applied Electrochemistry*, 20 pp. 672 (1990).
4. C. Y. CHAN, K. H. KHOO, Y. C. CHUA AND S. GURUSWAMY; *British Corrosion Journal*, 28 (1) pp. 53 (1993).
5. V. K. GOUDA, E. N. RIZKALLA, S. ABD EL-WAHAB AND E. M. IBRAHIM; *Corrosion Science*, 21 pp. 1 (1981).
6. A. EL-SAYED, F. H. ASSAF AND S. S. ABD EL- REHIM; *Hung. J. Ind. Chem.*, 19 (3) pp. 207 (1991).
7. B. F. GIANNETTI, P. T. A. SUMODJO, T. RABOCKAI, A. M. SOUZA AND J. BARBOZA; *Electrochimica Acta*, 37 pp. 143 (1992).
8. S. S. ABD EL-REHIM, S. M. SAYYAH AND M. M. EL- DEEB; *Materials Chemistry and Physics*, 80 (3) pp. 696 (2003).
9. S. S. ABD EL-REHIM, H. H. HASSAN AND F. N. MOHAMED; *Corrosion Science*, 46 (5) pp. 1071 (2004).
10. C. A. GERVASI, P.E. ALVAREZ, M.V. FIORI BIMBI AND M.E. FOLQUER; *Journal of Electroanalytical Chemistry*, 601 (1-2) pp. 194 (2007).
11. S. S. ABD EL REHIM, A. M. ZAKY AND N.F. MOHAMED; *Journal of Alloys and Compounds*, 424(1-2) pp. 88 (2006).
12. E. H. AIT ADDI, L. BAZZI, M. ELHILALI, Z.E. ALAMI, R. SALGHI AND S. E. ISSAMI; *Canadian Journal of Chemistry*, 81(4) pp. 297 (2003).
13. E.H. AIT ADDI, L. BAZZI, M. ELHILALI, R. SALGHI, B. HAMMOUTI AND M. MIHIT *Applied Surface Science*, 253(2) pp. 555 (2006).
14. D. PEREZ, F. SANZ AND P. GOROSTIZA; *Current Opinion in Solid state and Materials Science*, 10 (3- 4) pp. 144 (2007).
15. J. C. SHERLOCK AND S. C. BRITTON; *Br. Corrosion J.*, 7 pp. 180 (1972).
16. J. C. SHERLOCK AND S. C. BRITTON; *British Corrosion Journal*, 8 (5) pp. 210 (1973).
17. F. ASSAF, A. EL-SAYED, AND S. S. ABD EL- REHIM; *Bull. Electrochem.*, 7 pp. 207 (1991).
18. J. KRAGTEN; "Atlas of Metal Ligand Equilibria in Aqueous solutions", Elli Horwood, Chester, pp. 623 (1978).
19. M. S. ABD EL-AAL AND M. H. WAHDAN ; *Br. Corrosion J.*, 23 (1) pp. 25 (1988).
20. M. G. FONTANA; "Corrosion Engineering" MC Graw - Hill, (Chapter 6) pp. 222, 2nd ed. (1978).
21. M. A. QURAIISHI AND DANISH Jamal; *Materials Chemistry and Physics*, 78 pp. 608 (2003).
22. N. A. DARWISH, A. A. RAZIK, A. E. MAHGOUB, AND T. H. HUSSEIN; *Corros. Prev. Control*, 33(5) pp. 125 (1986).

الملخص العربي

السلوك الكهروكيميائي لقطب القصدير في بعض الأحماض العضوية

يتضمن البحث استعراض قياسات باستخدام طريقة الجهد الديناميكي المتغير على قطب القصدير في محاليل مختلفة التركيز من بعض الأحماض العضوية مثل حمض الستريك و الأوكساليك والطرطريك و الماليك و المالك.

تم أيضا دراسة تأثير اضافة بعض المواد الغير عضوية و العضوية (سترات ثلاثي الصوديوم , اوكسالات البوتاسيوم , السكروز, و كلوريد الصوديوم) على تآكل قطب القصدير في 1 مولار من كل من الأحماض العضوية المستخدمة في الدراسة و لقد تم التوصل للنتيجة التالية:

في حالة احمض الستريك و الطرطريك و الماليك و المالك وجد ان اضافة سترات ثلاثي الصوديوم أو اوكسالات البوتاسيوم أو السكروز, تعمل كمثبط مزدوج اي ان تأثيره على العمليات الأنودية مساويا لتأثيره على العمليات الكاثودية و ذلك نتيجة لامتزاز مركبات معقده SnL و الأمتزاز يتبع Temkin isotherm بينما في حالة حمض الأوكساليك يكون التثبيط آنودي و يحدث نتيجة لامتزاز المركبات المعقده SnL₂ وفي هذه الحالة تتبع Langmuir isotherm كما وجد ان لكلوريد الصوديوم تأثير ايجابي على تآكل الفلز حيث يزيد تآكل قطب القصدير بزيادة تركيز كلوريد الصوديوم .

وأوضحت نتائج الميكروسكوب الالكتروني الماسح لقطب القصدير في حمض الستريك و الأوكساليك في وجود و عدم وجود % 25 من السكروز تحسن سطح القطب و ان السكروز يكون طبقة حامية عن طريق الامتزاز على سطح القطب . و قد اوضحت النتائج ان الطبقة المتكونة في حالة حمض الأوكساليك الحر تكون ملتصقة (adherent) على سطح القطب بينما في حالة حمض الستريك تكون الطبقة مسامية (sponge).